

**INFLUENCE OF CRYSTAL ORIENTATION ON THE
CORROSION BEHAVIOUR OF COPPER,
ALUMINIUM AND NIOBIUM STUDIED USING
FIRST-PRINCIPLES CALCULATION**



YANG JUN
UMS
UNIVERSITI MALAYSIA SABAH

**FACULTY OF SCIENCE AND NATURAL RESOURCES
UNIVERSITI MALAYSIA SABAH**

2023

**INFLUENCE OF CRYSTAL ORIENTATION ON THE
CORROSION BEHAVIOUR OF COPPER,
ALUMINIUM AND NIOBIUM STUDIED USING
FIRST-PRINCIPLES CALCULATION**

YANG JUN



UMS

**THESIS SUBMITTED IN FULFILMENT OF THE
REQUIREMENTS FOR THE DEGREE OF
DOCTOR OF PHILOSOPHY**

**FACULTY OF SCIENCE AND NATURAL RESOURCES
UNIVERSITI MALAYSIA SABAH
2023**

UNIVERSITI MALAYSIA SABAH
BORANG PENGESAHAN STATUS TESIS

JUDUL : **INFLUENCE OF CRYSTAL ORIENTATION ON THE CORROSION BEHAVIOUR OF COPPER, ALUMINIUM AND NIOBIUM STUDIED USING FIRST-PRINCIPLES CALCULATION**

IJAZAH : **DOKTOR FALSAFAH SAINS GUNAAN**

BIDANG : **KIMIA INDUSTRI**

Saya **YANG JUN**, Sesi **2021-2023**, mengaku membenarkan tesis Doktor ini disimpan di Perpustakaan Universiti Malaysia Sabah dengan syarat-syarat kegunaan seperti berikut:-

1. Tesis ini adalah hak milik Universiti Malaysia Sabah
2. Perpustakaan Universiti Malaysia Sabah dibenarkan membuat salinan untuk tujuan pengajian sahaja.
3. Perpustakaan dibenarkan membuat salinan tesis ini sebagai bahan pertukaran antara institusi pengajian tinggi.
4. Sila tandakan (/):

SULIT

(Mengandungi maklumat yang berdarjah keselamatan atau kepentingan Malaysia seperti yang termaktub di dalam AKTA RAHSIA 1972)

TERHAD

(Mengandungi maklumat TERHAD yang telah ditentukan oleh organisasi/badan di mana penyelidikan dijalankan)

TIDAK TERHAD

Yang Jun

YANG JUN
DS2021012A

Disahkan Oleh,

AR ANITA BINTI ARSAD
PUSTAKAWAN KANAN
UNIVERSITI MALAYSIA SABAH

(Tandatangan Pustakawan)

Z

Tarikh : 26 September 2023

(Prof. Madya ChM. Dr. Moh Pak Yan)
Penyelia Utama

DECLARATION

I hereby declare that the material in this thesis is my own except for quotations, equations, summaries, and references, which have been duly acknowledged.

20 June 2023



YANG JUN
DS2021012A



UMMS
UNIVERSITI MALAYSIA SABAH

CERTIFICATION

NAME : **YANG JUN**
MATRIC NO. : **DS2021012A**
TITTLE : **INFLUENCE OF CRYSTAL ORIENTATION ON THE CORROSION BEHAVIOUR OF COPPER, ALUMINIUM AND NIOBIUM STUDIED USING FIRST-PRINCIPLES CALCULATION**
DEGREE : **DOCTOR OF PHILOSOPHY IN APPLIED SCIENCE**
FIELD : **INDUSTRIAL CHEMISTRY**
VIVA DATE : **20 June 2023**



CERTIFIED BY;

UMS
UNIVERSITI MALAYSIA SABAH

Signature

1. MAIN SUPERVISOR

Dr. Moh Pak Yan

A handwritten signature in black ink, appearing to read 'Moh Pak Yan', written over a horizontal line.

2. CO-SUPERVISOR

Dr. Saturi Baco

A handwritten signature in black ink, appearing to read 'Saturi Baco', written over a horizontal line.

ACKNOWLEDGEMENTS

I would like to express my gratitude to all those who helped me during my PhD studies.

First, I would like to express my deepest gratitude to my supervisor Dr. Moh Pak Yan, for his intellectual guidance, invaluable instructions, and comments on my thesis. He offered me many valuable suggestions in academic studies. In preparing this thesis, he has spent much time reading through each draft and provided me with inspiring advice. His constant patience and kind encouragement were the key towards the completion of my PhD study.

Special thanks should go to my co-supervisor Dr. Saturi Baco, her friendliness and carefulness have greatly helped me in my overseas studies, and her rigorous academic attitude has deeply influenced me.

I am also greatly indebted to Dr. Yongzhong Jin, he has given me many practical suggestions on topic selection and has provided such experimental equipment when I was unable to come to UMS during the COVID-19.

I am very grateful to my husband for his fully support in starting my PhD study. He has always encouraged me in the most difficult times. I would also like to thank my parents for their love, understanding, support, and encouragement until the completion of my PhD journey.

Lastly, I would like to thank Universiti Malyasia Sabah for giving me the chance to a further study. Thanks Sichuan University of Science and Engineering for providing experiment assistance.

YANG JUN

20 June 2023

ABSTRACT

Corrosion has an important impact on the properties of metal materials. Copper (Cu), aluminum (Al) and niobium (Nb) are widely used in many important fields because of their excellent properties. However, all the three metals are prone to corrosion. In study, the corrosion behaviour of Cu and Al were systematically studied by experimental methods, and the corrosion mechanisms were analyzed by First-principles Calculation. Subsequently, the results of Cu and Al obtained were employed to predict the corrosion resistance of Nb films with different crystal orientations. Firstly, the electrochemical method was used to illustrate the corrosion resistance of Cu and Al with (100), (110) and (111) surfaces in 3.5wt% NaCl, 0.1M H₂SO₄ and 0.1M NaOH solution, respectively. Both the electrochemical impedance spectroscopy (EIS) and polarization curve results revealed that crystal orientation has significant effect to the corrosion resistance of Cu and Al. The order of corrosion resistance for copper was Cu(110) > Cu(100) > Cu(111), and for aluminium was Al(100) > Al(110) > Al(111). Moreover, the corrosion resistance sequence of Cu and Al was the same in 3.5wt% NaCl, 0.1M H₂SO₄, and 0.1M NaOH solution, suggesting that the solution type has no impact on the crystal orientation affecting the corrosion resistance of Cu and Al. Secondly, the surface energy, work function, Mulliken charge population analysis and vacancy formation energy were calculated through First-principles calculation to reveal the corrosion mechanism. The calculation results showed that the Mulliken charge distribution was closely related to the corrosion resistance. A higher value of Mulliken charge led to a greater number of electrons participating in the electrochemical reaction, which in turn resulted in a poorer corrosion resistance. The electron number on each atom on Cu(100), Cu(110), Cu(111) plane was 11.04 e, 10.94 e and 11.14 e, respectively. And the values of Al(100), Al(110), Al(111) was 2.96 e, 2.91 e and 2.99 e, respectively. The Mulliken value order was (111) > (100) > (110), indicating the corrosion resistance sequence was (110) > (100) > (111) for both Cu and Al. In addition, due to the vacancy effect of Al, the vacancy formation energy of Cu(100), Cu(110), Cu(111) were 6.76 eV, 6.71 eV and 7.38 eV, respectively. While the values of Al(100), Al(110), Al(111) were 5.11 eV, 4.63 eV and 5.32 eV, respectively. It indicated that the vacancy was easier to form on the surface of Al than Cu. In the early stage of corrosion process, the corrosion resistance was Al(110) > Al(100) > Al(111), which was controlled by surface effect. In the late period, the corrosion resistance order changed to Al(100) > Al(110) > Al(111), which controlled by surface effect and vacancy effect. To predict the corrosion resistance of Nb with (100), (112), (110) and (120) planes, the surface energy, work function, Mulliken charge population analysis and vacancy formation energy were also calculated through First-principles calculation. Based on the analysis results of Cu and Al, the Mulliken charge distribution was used to predict the corrosion resistance of Nb. Results showed the values of Mulliken charge on the surface atom for the four structures were 13.18 e, 13.13 e, 13.19 e and 13.21 e. Therefore, the order of corrosion resistance for niobium will be Nb(112) > Nb(100) > Nb(110) > Nb(120). This study implies that the First-principles calculation by Mulliken charge analysis and vacancy formation energy analysis can be used to explain the corrosion mechanism metals in different solutions. Moreover, metal-corrosion data can be used to explain the important development trend of metals through simulation approach.

ABSTRAK

PENGARUH ORIENTASI KRISTAL TERHADAP TINGKAH LAKU KAKISAN TEMBAGA, ALUMINIUM DAN NIOBIUM YANG DIKAJI MENGGUNAKAN PENGIRAAN PRINSIP PERTAMA

Korrosi mempunyai kesan penting pada ciri-ciri bahan logam. Copper (Cu), aluminum (Al) dan niobium (Nb) digunakan secara luas di banyak bidang penting kerana ciri-ciri mereka yang baik. Namun, semua tiga logam itu susah untuk kerosakan. Dalam kajian, perilaku kerosakan Cu dan Al telah secara sistematik dipelajari dengan kaedah eksperimen, dan mekanisme kerosakan telah dianalisis dengan Kalkulasi prinsip pertama. Kemudian, hasil Cu dan Al yang diterima digunakan untuk meramalkan perlawanan kerosakan filem Nb dengan orientasi kristal yang berbeza. Pertama, kaedah elektrokimia digunakan untuk memperlihatkan perlawanan korosi Cu dan Al dengan (100), (110) dan (111) permukaan dalam 3,5 wt% NaCl, 0,1M H₂SO₄ dan 0,1M NaOH penyelesaian, berdasarkan. Kedua-dua spektroskopi impedance elektrokimia (EIS) dan hasil kurva polarisasi menunjukkan bahawa orientasi kristal mempunyai kesan yang signifikan terhadap perlawanan korosi Cu dan Al. Jadual perlawanan korosi untuk tembaga adalah Cu(110) > Cu(100) > Cu(111), dan aluminium adalah Al(100) > Al(110) > Al(111). Selain itu, urutan perlawanan korosi Cu dan Al adalah sama dalam 3.5 wt% NaCl, 0.1M H₂SO₄, dan 0.1M NaOH penyelesaian, menyarankan bahawa jenis penyelesaian tidak mempunyai kesan pada orientasi kristal yang mempengaruhi perlawanan korosi Cu dan Al. Kedua, tenaga permukaan, fungsi kerja, Analisis populasi muatan Mulliken dan tenaga pembentukan tempat kosong dihitung melalui pengiraan prinsip pertama untuk mengungkap mekanisme kerosakan. Hasil pengiraan menunjukkan bahawa distribusi muatan Mulliken berkaitan dengan perlawanan korosi. Nilai yang lebih tinggi muatan Mulliken membawa kepada bilangan elektron yang lebih besar yang berpartisipasi dalam reaksi elektrokimia, yang menurutnya mengakibatkan resistensi korrosi yang lebih buruk. Nombor elektron pada setiap atom pada kapal Cu(100), Cu(110), Cu(111) adalah 11.04 e, 10.94 e dan 11.14 e, respectively. Dan nilai Al(100), Al(110), Al(111) adalah 2.96 e, 2.91 e dan 2.99 e, respectively. Turutan nilai Mulliken adalah (111) > (100) > (110) untuk Cu dan Al, yang menunjukkan bahawa urutan perlawanan korosi adalah (110) > (100) > (111). Kerana kesan tempat kosong Al, tenaga formasi tempat kosong Cu(100), Cu(110), Cu(111) adalah 6.76 eV, 6.71 eV dan 7.38 eV, respectively. Sementara nilai Al(100), Al(110), Al(111) adalah 5.11 eV, 4.63 eV dan 5.32 eV, respectively. Ia menunjukkan bahawa tempat kosong adalah lebih mudah untuk membentuk di permukaan Al daripada Cu. Pada tahap awal proses korosi, perlawanan korosi adalah Al(110) > Al(100) > Al(111), yang dikawal oleh kesan permukaan. Dalam masa lewat, perintah perlawanan kerosakan berubah kepada Al(100) > Al(110) > Al(111), yang dikawal oleh kesan permukaan dan kesan kosong. Untuk meramalkan perlawanan korosi Nb dengan (100), (112), (110) dan (120) pesawat, tenaga permukaan, fungsi kerja, analisis populasi muatan Mulliken dan tenaga formasi kosong juga dihitung melalui pengiraan prinsip pertama. Berdasarkan hasil analisis Cu dan Al, distribusi muatan Mulliken digunakan untuk meramalkan perlawanan korosi Nb. Hasil menunjukkan nilai muatan Mulliken pada atom permukaan bagi empat struktur adalah 13.18 e, 13.13 e, 13.19 e dan 13.21 e. Oleh itu, tertib penentangan korosi untuk niobium akan Nb(112) > Nb(100) > Nb(110) > Nb(120). Kajian ini menunjukkan bahawa pengiraan prinsip-pertama oleh analisis muatan Mulliken dan analisis tenaga formasi kosong boleh digunakan untuk menjelaskan mekanisme kerosakan logam dalam penyelesaian yang berbeza. Selain itu, data kerosakan logam boleh digunakan untuk menjelaskan perkembangan penting logam melalui pendekatan simulasi.

LIST OF CONTENTS

	Page
TITLE	i
DECLARATION	ii
CERTIFICATION	iii
ACKNOWLEDGEMENT	vi
ABSTRACT	v
<i>ABSTRAK</i>	vi
LIST OF CONTENTS	vii
LIST OF TABLES	xi
LIST OF FIGURES	xiii
LIST OF ABBREVIATIONS	xix
LIST OF APPENDICES	xx
CHAPTER 1: INTRODUCTION	1
1.1 Background of the Study	1
1.2 Problem Statement	6
1.3 Objectives of the Study	7
1.4 Scope of Study	8
1.5 Summary	8
CHAPTER 2: LITERATURE REVIEW	9
2.1 Corrosion	9
2.1.1 Corrosion Definition	9
2.1.2 Corrosion Type	10
2.1.3 Corrosion Influence Factors	11
2.1.4 Corrosion Controlling Methods	14
2.1.5 Corrosion Characteristics of Copper	16
2.1.6 Corrosion Characteristics of Aluminium	18
2.1.7 Corrosion Characteristics of Niobium	20

2.2	Corrosion Test Methods	21
2.2.1	Basic Concept in Corrosion Test	21
2.2.2	Typical Corrosion Test Methods	29
2.3	Relation of Crystal Orientation	38
2.3.1	Unit Cells	39
2.3.2	Metallic Crystal Structures	40
2.3.3	Crystal Lattice, Crystallographic Directions, Crystallographic Planes	43
2.3.4	Single Crystals	45
2.3.5	Anisotropy	47
2.4	Current study on the Correlation between Corrosion and Crystal Orientation	48
2.4.1	The Correlation Between Metal Corrosion and Crystal Orientation	48
2.4.2	Current Studies on the Corrosion Behaviour of Single Crystal Cu with Different Planes	51
2.4.3	Current Studies on the Corrosion Behaviour of Single Crystal Al with Different Planes	53
2.4.4	Current Studies on the Fabrication of Single Crystal Nb Films with Different Planes	56
2.5	Overview of Simulation	58
2.5.1	Correlation of Experiment, Theory and Simulation	58
2.5.2	Main Simulation Method in Material Science	60
2.5.3	First-Principles Calculation	65
2.6	Current Studies on the Corrosion Behaviour of Single Crystal Cu, Al and Nb with Different Planes by First-principles Calculation	75
2.7	Summary	80
CHAPTER 3: METHODOLOGY		81
3.1	Research Design	81
3.2	Chemical and Reagent	82
3.2.1	Sample Sources	82

3.2.2	Solution Sources	84
3.3	Corrosion Test with Experimental Methods	84
3.3.1	Crystal Orientation Identification	84
3.3.2	Electrochemical Test	86
3.3.3	Surface morphology Test	89
3.4	Corrosion Mechanism with First-principles Calculation	90
3.4.1	Calculation Model	90
3.4.2	Calculation Software and Parameters	93
3.5	Summary	95
CHAPTER 4: EXPERIMENTAL RESULTS AND DISCUSSION		96
4.1	Effects of Crystal Orientation on the Corrosion Behaviour of Cu	96
4.1.1	Effects of Crystal Orientation on the Corrosion Behaviour of Cu in 3.5wt% NaCl Solution	96
4.1.2	Effects of Crystal Orientation on the Corrosion Behaviour of Cu in 0.1M H ₂ SO ₄ Solution	105
4.1.3	Effects of Crystal Orientation on the Corrosion Behaviour of Cu in 0.1M NaOH Solution	113
4.2	Effects of Crystal Orientation on the Corrosion Behaviour of Al	119
4.2.1	Effects of Crystal Orientation on the Corrosion Behaviour of Al in 3.5wt% NaCl Solution	119
4.2.2	Effects of Crystal Orientation on the Corrosion Behaviour of Al in 0.1M H ₂ SO ₄ Solution	126
4.2.3	Effects of Crystal Orientation on the Corrosion Behaviour of Al in 0.1M NaOH Solution	132
4.3	Summary	137
CHAPTER 5: SIMULATED RESULTS AND DISCUSSION		138
5.1	Assumptions Inferred from Experimental Results	138
5.2	Corrosion Mechanism of Cu(100), Cu(110) and Cu(111) with First-principles Calculation	140
5.2.1	Calculation Details	140

5.2.2	Calculation Results of Surface Structure	141
5.2.3	Calculation Results of Surface Properties	144
5.2.4	Discuss the Corrosion Mechanism of Cu(100), Cu(110) and Cu(111) with Calculated Results	147
5.3	Corrosion Mechanism of Al(100), Al(110) and Al(111) with First-principles Calculation	149
5.3.1	Calculation Details	149
5.3.2	Calculation Results of Surface Structure	150
5.3.3	Calculation Results of Surface Properties	151
5.3.4	Discuss the Corrosion Mechanism of Al(100), Al(110) and Al(111)	156
5.4	Predict the Corrosion Resistance of Nb films with Different Orientations by First-principles Calculation	158
5.4.1	Calculation Details	159
5.4.2	Calculation Results of Surface Structure	160
5.4.3	Calculation Results of Surface Properties	161
5.4.4	Predict the Corrosion Resistance of Nb films with Different Orientations	165
5.5	Summary	166
CHAPTER 6: CONCLUSION		167
6.1	Future Work	169
BIBLIOGRAPHY		170
APPENDICES		188

LIST OF TABLES

	Page
Table 2.1 : Difference between the Equilibrium Potential and Non-equilibrium Potential	25
Table 2.2 : Modulus of Elasticity Values for Several Metals at Various Crystallographic Directions	48
Table 2.3 : Examples of Corrosion Resistance with Different Orientations	49
Table 3.1 : Test Plans of Electrochemical Test Using OCP, EIS, Polarization Curve	88
Table 4.1 : Fitted EIS Data of Cu(100), Cu(110), Cu(111) in 3.5wt%NaCl Solution at 25°C.	100
Table 4.2 : Fitted Polarization Curves Parameters of Cu(100), Cu(110), Cu(111) in 3.5wt%NaCl Solution at 25°C.	102
Table 4.3 : Fitted EIS Data of Cu(100), Cu(110), Cu(111) in 0.1M H ₂ SO ₄ Solution at 25°C.	108
Table 4.4 : Fitted Polarization Curves Parameters of Cu(100), Cu(110), Cu(111) in 0.1M H ₂ SO ₄ Solution at 25°C.	110
Table 4.5 : Fitted EIS Data of Cu(100), Cu(110), Cu(111) in 0.1M NaOH Solution at 25°C.	115
Table 4.6 : Fitted Polarization Curves Parameters of Cu(100), Cu(110), Cu(111) in 0.1M NaOH Solution at 25°C.	116
Table 4.7 : Fitted EIS Data of Al(100), Al(110), Al(111) in 3.5wt% NaCl Solution at 25°C.	122
Table 4.8 : Fitted Polarization Curves Parameters of Al(100), Al(110), Al(111) in 3.5wt% NaCl Solution at 25°C.	124
Table 4.9 : Fitted EIS Data of Al(100), Al(110), Al(111) in 0.1M H ₂ SO ₄ Solution at 25°C.	128
Table 4.10 : Fitted Polarization Curves Parameters of Al(100), Al(110), Al(111) in 0.1M H ₂ SO ₄ Solution at 25°C.	129

Table 4.11	: Fitted EIS Data of Al(100), Al(110), Al(111) in 0.1M NaOH Solution at 25°C.	134
Table 4.12	: Fitted Polarization Curves Parameters of Al(100), Al(110), Al(111) in 0.1M NaOH Solution at 25°C.	135
Table 5.1	: Variation of Layer Spacing due to Structure Relaxation for Cu(100), Cu(110) and Cu(111), including the Change of Interlayer Distance (Δd , unit in Å), and the Corresponding Change Percentage ($\Delta d/d$).	143
Table 5.2	: Calculation Results of Cu(100), Cu(110), Cu(111)	148
Table 5.3	: Variation of Layer Spacing due to Structure Relaxation for Al(100), Al(110) and Al(111), including the Change of Interlayer Distance (Δd , unit in Å), and the Corresponding Change Percentage ($\Delta d/d$).	151
Table 5.4	: Calculation Results of Al(100), Al(110), Al(111)	156
Table 5.5	: Variation of Layer Spacing due to Structure Relaxation for Nb(100), Nb(112), Nb(110) and Nb(120), including the Change of Interlayer Distance (Δd , unit in Å), and the Corresponding Change Percentage ($\Delta d/d$).	161
Table 5.6	: Calculation Results of Nb(100), Nb(112), Nb(110) and Nb(120)	165

LIST OF FIGURES

	Page
Figure 1.1 : Serious Corrosion of Metals	2
Figure 2.1 : ORR Corrosion Process of Cu	18
Figure 2.2 : Schematic Diagram of Pitting Corrosion on Al Surface	19
Figure 2.3 : Schematic Diagram of Electrical Double Layers	23
Figure 2.4 : Schematic Diagram of Three-electrode System	26
Figure 2.5 : Schematic Diagram of Electrolytic Cell	27
Figure 2.6 : Potential Difference after Anodic Polarization and Cathodic Polarization	28
Figure 2.7 : Classification of Corrosion Measurement	30
Figure 2.8 : Schematic Diagram of Electrochemical Experiments Equipment	31
Figure 2.9 : EIS Diagram of (a) Nyquist Plots (b) Bode Plots	34
Figure 2.10 : Typical Equivalent Circuit Models	34
Figure 2.11 : Polarization Curve with Tafel Extrapolation Method	37
Figure 2.12 : 3x3x3 Cu Supercell with the Indication of Unit Cell	40
Figure 2.13 : Crystal Structure of Copper	41
Figure 2.14 : Crystal Structure of Aluminium	41
Figure 2.15 : Crystal Structure of Niobium	42
Figure 2.16 : Crystal Structure of HCP	43
Figure 2.17 : Unit Cell with X,Y,Z axes	44
Figure 2.18 : Schematic Diagram of (a) Atomic Arrangement and (b) Crystal Lattice	44
Figure 2.19 : Crystal Directions with [100], [110], [111]	45
Figure 2.20 : Crystal Planes with (100), (110) and (111)	45
Figure 2.21 : Structure of (a)Single Crystal, (b)Polycrystalline	46
Figure 2.22 : Corrosion Rate vs. Corrosion Time of Single Crystal Cu and Polycrystalline Cu in 3.5% NaCl Solution	47
Figure 2.23 : Natural Corrosion Form of Different Crystal Orientation in 3.5 wt% Sodium Chloride Solution after 30 days	52

Figure 2.24	: SEM Micrographs of Al Surface Pitted in 1M HCl Solution. (a) {111}Surface Pitted by Pulsed dc Waveform, (b) {111}Surface Pitted by dc Waveform, (c) {110}Surface Pitted by dc Waveform, and (d) {100}Surface Pitted by dc Waveform.	53
Figure 2.25	: Atom Distributions at the Specimen Surface for Al	54
Figure 2.26	: SEM Images of Corrosion Morphology of Pure Al with: (a) (100), (b) (110) and (c) (111) Preferred Orientation, after Potentiodynamic Polarization Measurement for 0.5 h in 3.5wt% NaCl Solution	54
Figure 2.27	: The Average Number of Metastable Pitting Events/cm ² min vs. Potential for Single Crystals with Orientations of (100), (110) and (111).	55
Figure 2.28	: TEM and XRD Results of Nb/MgO(100) and Nb/MgO(111) System	57
Figure 2.29	: The Growth Orientation of Niobium Films on Quartz Substrate under Different Depositing Temperatures.	58
Figure 2.30	: The Relationship between Experiment, Theory and Simulation in Material Science Research	59
Figure 2.31	: Simulation Methods at Different length Scales and Time Scales	60
Figure 2.32	: Schematic Diagram of Work Function	73
Figure 2.33	: Schematic Diagram of Change Difference with Binding Electron Density around a Single Al Atom along [100],[110] and [111] Principal Direction	76
Figure 2.34	: The Neighbors Arrangement of Cu Atom in Bulk, (111) Face, (200) Face and (220) Face	77
Figure 2.35	: Al ₂ Cu(100) Slab Model and the Calculation Results of Electrostatic Potential Curves	77
Figure 2.36	: Calculation Results of Interface Separation Work for Nb/MgO Systems	79
Figure 3.1	: Schematic Diagram of Research Design	82
Figure 3.2	: Electrochemical Sample Pictures of (a) Cu and (b) Al	83
Figure 3.3	: Immersion Sample Pictures of (a) Cu and (b) Al	83
Figure 3.4	: Schematic Diagram of XRD Theory	85
Figure 3.5	: Instrument of XRD	85

Figure 3.6	: Instrument of Electrochemical Work Station	86
Figure 3.7	: Three-electrode System	86
Figure 3.8	: Flow Chart of Electrochemical Test	87
Figure 3.9	: Immersion Test	89
Figure 3.10	: Schematic Diagram of FESEM Theory	89
Figure 3.11	: Instrument of FESEM	90
Figure 3.12	: Schematic Diagram of Building Model Process	91
Figure 3.13	: Schematic Diagram of Slab Model for Cu(100)	92
Figure 3.14	: Schematic Diagram of Periodic Boundary Conditions	92
Figure 3.15	: Convergence Test of Calculation Parameters, including Layer number, Cut-off Energy and K point	94
Figure 4.1	: XRD Results of Cu(100), Cu(110) and Cu(111)	97
Figure 4.2	: EIS Diagram of Cu(100), Cu(110), Cu(111) in 3.5wt%NaCl Solution at 25°C. (a) Nyquist Plots, (b) Bode Plots	97
Figure 4.3	: The Equivalent Circuit Corresponding to EIS Plots for Cu(100), Cu(110), Cu(111) in 3.5wt%NaCl Solution at 25°C.	99
Figure 4.4	: Polarization Curves of Cu(100), Cu(110), Cu(111) in 3.5wt% NaCl Solution at 25°C.	102
Figure 4.5	: FESEM of Cu(100), Cu(110), Cu(111) in 3.5wt%NaCl Solution at 25°C for 24hours.	104
Figure 4.6	: EIS Diagram of Cu(100), Cu(110), Cu(111) in 0.1M H ₂ SO ₄ Solution at 25°C. (a) Nyquist Plots, (b) Bode Plots.	106
Figure 4.7	: The Equivalent Circuit Corresponding to EIS plots for Cu(100), Cu(110), Cu(111) in 0.1M H ₂ SO ₄ Solution at 25°C.	107
Figure 4.8	: Polarization Curves of Cu(100), Cu(110), Cu(111) in 0.1M H ₂ SO ₄ Solution at 25°C.	109
Figure 4.9	: FESEM of Cu(100), Cu(110), Cu(111) in 0.1M H ₂ SO ₄ Solution at 25°C for 24hours.	111
Figure 4.10	: EIS Diagram of Cu(100), Cu(110), Cu(111) in 0.1M NaOH Solution at 25°C. (a) Nyquist Plots, (b) Bode	113

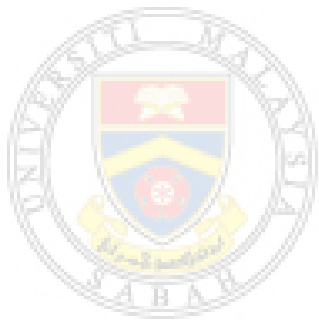
	Plots.	
Figure 4.11	: The Equivalent Circuit Corresponding to EIS plots for Cu(100), Cu(110), Cu(111) in 0.1M NaOH Solution at 25°C.	114
Figure 4.12	: Polarization Curves of Cu(100), Cu(110), Cu(111) in 0.1M NaOH Solution at 25°C.	116
Figure 4.13	: FESEM of Cu(100), Cu(110), Cu(111) in 0.1M NaOH Solution at 25°C for 24hours.	118
Figure 4.14	: XRD Results of Al(100), Al(110) and Al(111)	120
Figure 4.15	: EIS Diagram of Al(100), Al(110), Al(111) in 3.5wt% NaCl Solution at 25°C. (a) Nyquist Plots, (b) Bode Plots.	120
Figure 4.16	: The Equivalent Circuit Corresponding to EIS plots for Al(100), Al(110), Al(111) in 3.5wt% NaCl Solution at 25°C.	122
Figure 4.17	: Polarization Curves of Al(100), Al(110), Al(111) in 3.5wt%NaCl Solution at 25°C.	123
Figure 4.18	: FESEM of Al(100), Al(110), Al(111) in 3.5wt%NaCl Solution at 25°C for 24hours.	125
Figure 4.19	: EIS Diagram of Al(100), Al(110), Al(111) in 0.1M H ₂ SO ₄ Solution at 25°C. (a) Nyquist Plots, (b) Bode Plots.	127
Figure 4.20	: The Equivalent Circuit Corresponding to EIS plots for Al(100), Al(110), Al(111) in 0.1M H ₂ SO ₄ Solution at 25°C.	127
Figure 4.21	: Polarization Curves of Al(100), Al(110), Al(111) in 0.1M H ₂ SO ₄ Solution at 25°C.	129
Figure 4.22	: FESEM Images of Al(100), Al(110), Al(111) in 0.1M H ₂ SO ₄ Solution at 25°C for 24hours.	131
Figure 4.23	: EIS Diagram of Al(100), Al(110), Al(111) in 0.1M NaOH Solution at 25°C. (a) Nyquist Plots, (b) Bode Plots.	133
Figure 4.24	: The Equivalent Circuit Corresponding to EIS Plots for Al(100), Al(110), Al(111) in 0.1M NaOH Solution at 25°C.	133
Figure 4.25	: Polarization Curves of Cu(100), Cu(110), Cu(111) in 0.1M NaOH Solution at 25°C.	135
Figure 4.26	: FESEM of Al(100), Al(110), Al(111) in 0.1M NaOH	136

Solution at 25°C for 24hours.

Figure 5.1	: Crystal Structure of Cu with (100), (110), (111) Planes	140
Figure 5.2	: Slab Models of Cu(100), Cu(110) and Cu(111)	141
Figure 5.3	: Calculation Results of Density of State for Bulk Cu	142
Figure 5.4	: Structure Relaxation for Cu(100), Cu(110) and Cu(111) Slab Models	143
Figure 5.5	: Calculation Results of Work Function for Cu(100), Cu(110) and Cu(111)	145
Figure 5.6	: Atomic Mulliken Charge Analysis for Cu(100), Cu(110) and Cu(111) Slabs	146
Figure 5.7	: Calculation Results of Electron Density Difference for Cu(100), Cu(110) and Cu(111) Slabs	147
Figure 5.8	: Crystal Structure of Al(100) 4×4 Supercell with One Vacancy	149
Figure 5.9	: Calculation Results of Density of State for Bulk Al	150
Figure 5.10	: Structure Relaxation for Al(100), Al(110) and Al(111) Slab Models	151
Figure 5.11	: Calculation Results of Work Function for Al(100), Al(110) and Al(111) Slabs	152
Figure 5.12	: Atomic Mulliken Charge Analysis for Al(100), Al(110) and Al(111) Slabs.	153
Figure 5.13	: Calculation Results of Electron Density Difference for Al(100), Al(110) and Al(111) Slabs.	154
Figure 5.14	: Vacancy Effect on the Electron Distribution on Al(100), Al(110) and Al(111) Surfaces.	155
Figure 5.15	: Surface Effect and Vacancy Effect on the Electron Distribution	156
Figure 5.16	: Schematic Diagram of Relative Corrosion Resistance of Al(100), Al(110) and Al(111)	157
Figure 5.17	: Calculation Results of Interface Separation Work for Twenty-nine Nb/MgO(112) Calculation Models	158
Figure 5.18	: Slab Models of Nb(100), Nb(112), Nb(110) and Nb(120)	159
Figure 5.19	: Calculation Results of Density of State for Bulk Nb	160
Figure 5.20	: Structure Relaxation for Nb(100), Nb(112), Nb(110)	161

and Nb(120)

- Figure 5.21 : Calculation Results of Work Function for Nb(100), Nb(112), Nb(110) and Nb(120) Slabs 162
- Figure 5.22 : Atomic Mulliken Charge Analysis for Nb(100), Nb(112), Nb(110) and Nb(120) 163
- Figure 5.23 : Vacancy Effect on the Electron Distribution on (a) Nb(100), (b) Nb(112), (c) Nb(110) and (d) Nb(120) 164



UMS
UNIVERSITI MALAYSIA SABAH

LIST OF ABBREVIATIONS

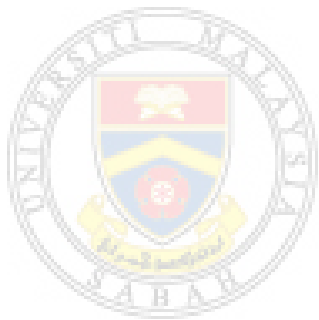
Cu	- Copper
Al	- Aluminium
Nb	- Niobium
OCP	- Open Circuit Potential
EIS	- Electrochemical Impedance Spectroscopy
SCE	- Saturated Calomel Electrode
XRD	- X-ray Diffraction
FESEM	- Field Emission Scanning Electron Microscope
GGA	- Generalized Gradient Approximation
LDA	- Local Density Approximation
DFT	- Density Functional Theory
ORR	- Oxygen Reduction Reaction
HER	- Hydrogen Evolution Reaction
FCC	- Face Centered Cubic
BCC	- Body Centered Cubic
HCP	- Close-Packed Hexagonal
PBC	- Periodic Boundary Conditions



UMS
UNIVERSITI MALAYSIA SABAH

LIST OF APPENDICES

	Page
Appendix A : Calculation Parameters Test for Cu Clab Model	188
Appendix B : Calculation Parameters Test for Al Clab Model	189
Appendix C : Calculation Parameters Test for Nb Clab Model	190



UMS
UNIVERSITI MALAYSIA SABAH

CHAPTER 1

INTRODUCTION

1.1 Background of the Study

Metallic materials have become an important basis for the development of human society (Johnson, 2009; Tao et al., 2007). Among all the metal materials, copper (Cu), aluminium (Al) and niobium (Nb) are widely used because of their excellent properties. Cu has the excellent thermal conductivity, electrical conductivity, and ductility (Xiao, 2021; Jmiai et al., 2018). Al possesses several fascinating properties, such as good electrical and thermal conductivity, low density and easy to process (Lucente, 2008; Cao et al., 2005). Nb has the characteristics of high melting point and high mechanical strength (Wang & Alfantazi, 2015; Gontad et al., 2016; De Freitas et al., 2016). All the three metals and their alloys are widely used in transportation, machinery, industries fields, etc.

However, corrosion is likely to occur under high humidity or typical types of solutions, such as seawater, acidic or alkaline solutions (Kang, 2010). Corrosion refers to the phenomenon that the material transforms into a new phase, suffers damage, and loses its inherent properties due to harmful chemical, electrochemical or physical changes in the surrounding environment (Johnson, 2009). The free energy of the corrosion system decreases when the corrosion occurs. The serious corrosion metals are shown in Figure 1.1.

Corrosion is a serious problem in nearly every industry. Solving or delaying the corrosion rate of metal materials is a big challenge. Revealing the corrosion mechanism and improving the corrosion resistance are significant in material fields.

To investigate the corrosion mechanism, it is advisable to initiate the study by focusing on the factors that contribute to corrosion.



Figure 1.1 : Serious Corrosion of Metals

Many factors may cause the metal corrosion, like the environmental factors (such as the concentration, pH, temperature, pressure, etc.), the surface state of metal (about the dust, oil, water, oxide skin, rust and other surface defects). While the main factor attributes to the inner microstructure of the metal (Liu & Shang 2021b; Martinez-Lombardia et al., 2014; Hagihara et al., 2016; Yang et al., 2020). Many studies are focusing on the effect of crystal orientation on metal corrosion in recent years (Zbigniew et al., 2015; Song & Xu, 2012, Lopez-Sesenes et al., 2018; Zhu et al., 2022). They proposed that the corrosion behaviour was correlated with grains and orientation-dependent. Feng Wen investigated the effect of crystal orientations and precipitates on the corrosion behaviour of the Al-Cu alloy using single crystals, they viewed that the corrosion resistance of the alloy without precipitates was mainly determined by the atomic density of the crystal plane (Wen et al., 2022). Studying the corrosion mechanism of metal materials from crystal structure field is a good way to guide us designing more advanced corrosion-resistant materials.

As single crystal structure refers the atoms with regular arrangement and no grain boundaries to accelerate corrosion, many investigations choose the single crystal materials to investigate the correlation between the crystal orientation and corrosion behaviour (Zhu et al., 2022; Song et al., 2010; Seo et al., 2003). For Cu, Masatoshi Sugimasa, Fang, et al. try to reveal the corrosion mechanism through